

Satellite-derived Ecosystem Functional Types capture ecosystem functional heterogeneity at regional scale

Beatriz P. Cazorla^{1,2*}, Ana Mejjide³, Javier Cabello^{1,4}, Julio Peñas^{1,5}, Rodrigo Vargas⁶, Javier Martínez-López^{1,2,7}, Leonardo Montagnani⁸, Alexander Knohl⁹, Lukas Siebicke⁹, Benimiano Gioli¹⁰, Jiří Dušek¹¹, Ladislav Šigut¹¹, Andreas Ibrom¹², Georg Wohlfahrt¹³, Eugénie Paul-Limoges¹⁴, Kathrin Fuchs¹⁵, Antonio Manco¹⁶, Marian Pavelka¹¹, Lutz Merbold¹⁷, Lukas Hörtnagl¹⁸, Pierpaolo Duce¹⁰, Ignacio Goded¹⁹, Kim Pilegaard¹², Domingo Alcaraz-Segura^{1,2,4}

¹Andalusian Center for Global Change – Hermelindo Castro (ENGLIBA), University of Almería, 04120 Almería, Spain.

²Interuniversity Institute of Earth System Research in Andalusia (IISTA), 18006 Granada, Spain.

³Environment Modeling, Institute of Crop Science and Resource Conservation, University of Bonn, Niebuhrstraße 1a, 53113 Bonn, Germany.

⁴Department of Biology and Geology, University of Almería, 04120 Almería, Spain.

⁵Department of Botany, University of Granada, 18006 Granada, Spain.

⁶School of Life Sciences, Arizona State University, Tempe, AZ, USA.

⁷Department of Ecology, University of Granada, 18006 Granada, Spain.

⁸Faculty of Agricultural, Environmental and Food Sciences, Free University of Bolzano, Italy.

⁹University of Goettingen, Bioclimatology, Büsgenweg 2, 37077 Göttingen, Germany.

¹⁰CNR – IBE, Institute of Bioeconomy, Firenze, Italy.

¹¹Department of Matters and Energy Fluxes, Global Change Research Institute CAS, Brno, Czech Republic.

¹²Department of Resource and Environmental Engineering, Technical University of Denmark, Kongens Lyngby, Denmark.

¹³Department of Ecology, University of Innsbruck, Innsbruck, Austria.

¹⁴Department of Geography, University of Zurich, Switzerland.

¹⁵Karlsruhe Institute of Technology, Institute of Meteorology and Climate Research - Atmospheric Environmental Research, Garmisch-Partenkirchen, Germany.

¹⁶Institute for Agriculture and Forestry Systems in the Mediterranean (ISAFoM), National Research Council of Italy, P.le E. Fermi 1-Loc, Porto del Granatello 1, 80055 Portici, Italy.

¹⁷Department of Agroecology and Environment, Reckenholzstrasse 191, 8046 Zurich, Switzerland.

¹⁸Department of Environmental System Science, Institute of Agricultural Science, Zurich, Switzerland.

¹⁹European Commission, Joint Research Centre, Ispra, Italy.

Correspondence to: Beatriz P. Cazorla (b.cazorla@ugr.es)

Abstract. Assessing ecosystem functioning is crucial for managing and conserving ecosystems and their services. Numerous ways to evaluate ecosystem functioning have been developed, using species traits, such as Plant Functional Types (PFTs), flux measurements with the Eddy Covariance (EC) technique, and remote sensing techniques. We propose that the spatial heterogeneity in ecosystem functioning at a regional scale can be assessed and monitored using satellite-derived Ecosystem Functional Types (EFTs): groups of ecosystems or patches of the land surface that share similar dynamics of matter and energy exchanges. We hypothesize that, as observed for PFTs, different EFTs should have distinct patterns and magnitudes of Net Ecosystem Exchange (NEE) of carbon dioxide measured using the EC technique. We derived EFTs from 2001-2014 time-series of satellite images of the Enhanced Vegetation Index (EVI) and compared them with NEE measurements (derived from

40 in situ field observations using the EC technique) across 50 European sites. Our results show that distinct EFTs classes display
41 significantly different dynamics and magnitudes of NEE and that EFTs perform marginally better than PFTs in explaining
42 NEE regional patterns. Land-cover maps based on PFTs are difficult to update on an annual basis and are not sensitive to
43 changes in ecosystem performance (e.g., droughts or pests) that do involve short-term changes in PFT composition. In contrast,
44 satellite-derived EFTs are sensitive to short-term changes in ecosystem performance. Satellite-derived EFTs are an ecosystem
45 functional classification built from satellite observations that allow the identification of homogeneous land patches based on
46 ecosystem functions, e.g., ecosystem net productivity measured on the ground as NEE. Satellite-derived EFTs can be
47 recalculated annually, providing a straightforward way to assess and monitor interannual changes in ecosystem functioning
48 and functional diversity.

49 **1 Introduction**

50 Ecosystem functioning and functional diversity are critical issues in current ecological research (Jax, 2010; Violle et al. 2014,
51 2017; Tilman et al. 2014; Pettoirelli et al. 2018; Villarreal et al. 2018; Malaterre et al. 2019; Díaz et al. 2020). Quantifying,
52 monitoring, and understanding ecosystem functioning help provide insights into the management and conservation of
53 ecosystems and their services (Cabello et al. 2012; Pettoirelli et al. 2018; Nicholson et al. 2021). Variables capable of describing
54 ecosystem functioning at regional to global scales are needed to define essential biodiversity variables to monitor biodiversity
55 status (Pereira et al. 2013; Jetz et al. 2019), to advance in the definition of critical but still unassessed planetary boundary
56 (Steffen et al. 2015; Richardson et al. 2023), and to quantify their associated ecosystem services (Costanza et al. 1997;
57 Balvanera et al. 2017).

58 There are multiple ways to evaluate ecosystem functioning, from concepts such as species traits or Plant Functional Types
59 (PFTs) to direct observation techniques such as eddy covariance (EC) and remote sensing. Traditionally, studies on ecosystem
60 functioning were approached by grouping species into PFTs based on structural (e.g., biotypes), phylogenetic (e.g.,
61 coniferous), or functional species traits (e.g., metabolic pathway) that were linked to biological processes (Lavorel et al. 2002,
62 2007). For instance, the PFT approach has been widely used in land-cover mapping and dynamic vegetation models to simplify
63 the continuum of species traits into a reduced number of discrete categories suitable for regional-to-global synthesis and
64 modeling studies (Wullschleger et al. 2014). However, this simplification can lead to information loss (Funk et al. 2017) and
65 may not be capable of predicting the overall ecosystem functioning (Virtanen, 2017; Thomas et al. 2019). Another more recent
66 way to evaluate ecosystem functioning is by using EC (Reichstein et al. 2014; Migliavacca et al. 2021). EC uses high-frequency
67 wind and scalar mixing ratio data for calculating the Net Ecosystem CO₂ Exchange (NEE) between the land surface and the
68 atmosphere at the field scale (Baldocchi et al. 2001, 2020). This approach is widely used and regional (e.g., AmeriFlux,
69 AsiaFlux, ICOS, NEON), and a global network of EC measurements has been formed (e.g., FLUXNET) (Franz et al. 2018;
70 Knox et al. 2019). Although FLUXNET has provided unprecedented information on the carbon, water, and energy exchange
71 between the earth's surface and the atmosphere, these measurements still show limitations to assessing ecosystem functioning

72 at regional or global scales due to their small footprints (essentially considered as point-scale data (Chu et al. 2021) and a lack
73 of spatial representativity (Villarreal et al. 2018, 2021). In parallel, advances in remote sensing are providing new opportunities
74 to quantify ecosystem functioning and functional diversity from regional to global scales (Rocchini et al. 2018; Skidmore et
75 al. 2021). Consequently, combining field-based measurements (e.g., EC) with remote sensing data may allow for better
76 information integration across multiple spatial and temporal scales (Running et al. 1999; Wang et al. 2017). Indeed, multiple
77 studies have aimed to derive global maps combining flux measurements with earth observation data, although challenges and
78 limitations still need to be addressed (e.g., FLUXCOM; Huang et al. 2019; Jung et al. 2020; Liu et al. 2023; Pacheco-Labrador
79 et al. 2023; Gomasasca et al. 2024; Nelson et al. 2024).

80 Ecosystem functioning and functional diversity at the regional scale can be assessed using satellite-derived Ecosystem
81 Functional Types (EFTs) (Paruelo et al. 2001). Conceptually, EFTs are defined as patches of the land surface that share similar
82 dynamics of matter and energy exchanges between the biota and the physical environment (Alcaraz-Segura et al. 2006, 2013;
83 Cazorla et al. 2020, 2021, 2023). The concept of EFT is equivalent to the concept of PFTs but applied to a higher level of
84 biological organization. That is, just like plant species can be grouped based on shared functional traits (e.g., growth rates,
85 nitrogen fixation) into PFTs, ecosystems can be grouped based on their common functional dynamics (e.g., productivity,
86 seasonality, phenology) into EFTs (Paruelo et al. 2001). Remote sensing has been empirically applied to identify EFTs, mainly
87 through spectral indices related to carbon dynamics (Paruelo et al., 2001; Alcaraz-Segura et al., 2006; Ivits et al., 2013), but
88 also incorporating other functional attributes such as evapotranspiration, surface temperature, and albedo (e.g., Fernández et
89 al. 2010; Pérez-Hoyos et al. 2014) or soil characteristics based on their greenhouse gas flux dynamics (Petraakis et al. 2018).
90 Among these functional attributes, those linked to carbon dynamics, particularly primary production, represent one of the most
91 integrative dimensions of ecosystem functioning because they reflect the main entry of energy into ecosystems and are directly
92 related to key carbon and energy exchanges (Virginia and Wall 2001; Pereira et al. 2013; Xiao et al. 2019). Moreover, primary
93 production provides a holistic response to environmental changes and constitutes a synthetic indicator of ecosystem health
94 (Costanza et al. 1992; Skidmore et al. 2015). Other authors have used EFTs to: describe large-scale functional biogeographical
95 patterns (Ivits et al. 2013; Cazorla et al. 2021), assess the representativeness of environmental observatory networks (Villarreal
96 et al. 2018, 2019), assess the ecosystem functional diversity (Alcaraz-Segura et al. 2013; Liu et al. 2023; Armstrong et al. 2024),
97 evaluate the effects of land-use changes on ecosystem functioning (Oki et al. 2012; Domingo-Marimon et al. 2024), improve
98 weather forecasting (Lee et al. 2013; Müller et al. 2014) and species distribution/abundance models (Arenas-Castro et al. 2018,
99 2019), and to identify geographic priorities for biodiversity conservation (Cazorla et al. 2020).

100 So far, EFTs have been identified from satellite remote sensing data. However, whether such top-down-identified EFT classes
101 are biologically meaningful in ecological processes measured on the ground, such as biogeochemical fluxes, remains untested.
102 That is, whether satellite-derived EFT classes differ in their exchanges of energy and matter between ecosystems and the
103 atmosphere. Therefore, linking satellite-derived EFTs identified at large scales to biogeochemical fluxes measured at the site
104 level could help strengthen the ecological significance of the EFT patterns for ecosystem modeling and functional diversity
105 assessments remotely, as it provides empirical evidence for using the concept at these scales.

106 This study aims to provide field-based empirical evidence for using satellite-derived EFTs as descriptors of regional
 107 heterogeneity in ecosystem functioning measured on the ground (i.e., seasonal dynamics of NEE). We hypothesize that
 108 satellite-derived EFTs classes significantly differ in their exchanges of energy and matter with the atmosphere from each other,
 109 in the same way as estimated with in situ field observations. Here, we propose that different satellite-derived EFTs classes
 110 display significantly different NEE measurements using the EC technique, while sites under the same EFT should exhibit
 111 similar NEE dynamics. To achieve our goal, we used publicly available data across continental Europe, given its high density
 112 of EC sites, 1) to characterize the regional patterns of ecosystem functioning using satellite-derived EFTs; 2) to assess whether
 113 different satellite-derived EFTs correspond to different NEE dynamics measured on the ground with the EC technique; and 3)
 114 to assess how EFTs perform compared to traditional PFTs to discriminate different NEE dynamics.

115 2 Material and methods

116 2.1 Study area

117 We used NEE information from continental Europe as it has one of the largest densities of EC sites worldwide (Table 1). The
 118 sites were distributed across four biogeographical regions (EEA 2016): Mediterranean (12 sites), Continental (21 sites),
 119 Atlantic (9 sites), and Alpine (8 sites). Only sites with a long-term (i.e., from 3 to 14 years) NEE time-series were included in
 120 the analysis (detailed below).
 121

122 **Table 1.** Main characteristics of the 50 Eddy Covariance (EC) sites in the study area. Data from FLUXNET 2015 dataset.

ID	Site	Country	PFT	EFT code	Biogeographical region	n years (2001-2014)	Elevation (m)	Latitude	Longitude
AT-Neu	Neustift/ Stubai Valley	Austria	Grasslands	Da2	Alpine	11 (2002-2013)	970	47.116	11.317
BE-Bra	Brasschaat (De Inslag Trees)	Belgium	Mixed Trees	Cc1	Atlantic	14 (2001-2014)	16	51.309	4.520
BE-Lon	Lonze	Belgium	Croplands	Ba1	Atlantic	11 (2004-2014)	167	50.552	4.744
BE-Vie	Vielsalm	Belgium	Mixed Trees	Bc1	Continental	14 (2001-2014)	439	50.305	5.998
CH-Cha	Chamau grassland	Switzerland	Grasslands	Db1	Continental	10 (2005-2014)	393	47.210	8.410
CH-Dav	Davos-	Switzerland	Evergreen	Ac2	Alpine	14 (2001-2014)	1639	46.815	9.855

	Seehorn forest		Needleleaf Trees						
CH-Fru	Fruebuel grassland	Switzerland	Grasslands	Da2	Continental	10 (2005-2014)	982	47.115	8.537
CH-Lae	Laegeren	Switzerland	Mixed Trees	Da1	Continental	11 (2004-2014)	689	47.478	8.365
CH-Oe1	Oensingen1 grass	Switzerland	Croplands	Cb1	Continental	7 (2002-2008)	450	47.285	7.731
CH-Oe2	Oensingen2 crop	Switzerland	Croplands	Cb1	Continental	11 (2004-2014)	452	47.286	7.733
CZ-BK1	Bily Kriz-Beskidy Mountains	Czech Republic	Evergreen Needleleaf Trees	Cc1	Continental	11 (2004-2014)	875	49.502	18.536
CZ-BK2	Bily Kriz-grassland	Czech Republic	Grasslands	Ac1	Alpine	9 (2004-2012)	855	49.494	18.542
CZ-wet	CZECH WET	Czech Republic	Wetlands	Ba1	Continental	9 (2004-2012)	426	49.024	14.770
DE-Akm	Anklam	Germany	Wetlands	Ba1	Continental	5 (2010-2014)	-1	53.866	13.683
DE-Geb	Gebesee	Germany	Croplands	Ba1	Continental	14 (2001-2014)	161	51.100	10.914
DE-Gri	Grillenburger-grass station	Germany	Grassland	Da2	Continental	11 (2004-2014)	385	50.949	13.512
DE-Hai	Hainich	Germany	Mixed Trees	Ca1	Continental	12 (2001-2012)	430	51.079	10.452
DE-Kli	Klingenberg	Germany	Croplands	Ba1	Continental	11 (2004-2014)	478	50.892	13.522
DE-Lkb	Lackenberger	Germany	Evergreen Needleleaf Trees	Ab2	Continental	5 (2009-2013)	1308	49.099	13.304
DE-Lnf	Leinefelde	Germany	Deciduous Broadleaf Trees	Da1	Continental	11 (2002-2012)	451	51.328	10.367
DE-Obe	Oberbärenburg	Germany	Evergreen Needleleaf	Ac1	Continental	7 (2008-2014)	734	50.786	13.721

			Trees						
DE-RuR	Rollesbroich	Germany	Grasslands	Da2	Continental	4 (2011-2014)	515	50.621	6.304
DE-RuS	Selhause n Juelich	Germany	Croplands	Cb1	Atlantic	4 (2011-2014)	103	50.865	6.447
DE-Seh	Selhause n	Germany	Croplands	Cb1	Atlantic	4 (2007-2010)	103	50.870	6.449
DE-Spw	Spreewal d	Germany	Mixed Trees	Ca1	Continental	5 (2010-2014)	61	51.892	14.033
DE-Tha	Tharandt- Anchor Station	Germany	Evergreen Needleleaf Trees	Bc1	Continental	14 (2001-2014)	385	50.963	13.566
DK-Eng	Enghave	Denmark	Croplands	Ca1	Continental	4 (2005-2008)	10	55.690	12.191
DK-Sor	Soroelille- LilleBog skov	Denmark	Deciduous Broadleaf Trees	Da1	Continental	14 (2001-2014)	40	55.485	11.644
ES-Amo	Amolader as	Spain	Shrublands	Ad4	Mediterran ea	6 (2007-2012)	58	36.833	-2.252
ES-LJu	Llano de los Juanes	Spain	Shrublands	Ad1	Mediterran ea	10 (2004-2013)	1600	36.926	-2.752
FR-Fon	Fontaineb leau	France	Deciduous Broadleaf Trees	Da1	Atlantic	10 (2005-2014)	103	48.476	2.780
FR-Gri	Grignon	France	Croplands	Cc1	Atlantic	11 (2004-2014)	125	48.844	1.951
FR-LBr	Le Bray	France	Cropland	Cd1	Atlantic	8 (2001 - 2008)	61	44.717	-0.769
FR-Pue	Puechabo n	France	Mixed Trees	Cd1	Mediterran ea	14 (2001-2014)	270	43.741	3.595
IT-BCi	Borgo Cioffi	Italy	Croplands	Db4	Mediterran ea	11 (2004-2014)	20	40.523	14.957
IT-CA1	Castel d'Asso1	Italy	Croplands	Bd1	Mediterran ea	4 (2011-2014)	200	42.380	12.026
IT-CA2	Castel d'Asso2	Italy	Croplands	Cb1	Mediterran ea	4 (2011-2014)	200	42.377	12.026

IT-CA3	Castel d'Asso 3	Italy	Croplands	Bd1	Mediterran ea	4 (2011-2014)	197	42.380	12.022
IT-Col	Collelong o- Selva Piana	Italy	Deciduous Broadleaf Trees	Da1	Alpine	14 (2001-2014)	1560	41.849	13.588
IT-Cpz	Castelpor ziano	Italy	Evergreen Needleleaf Trees	Dd1	Mediterran ea	9 (2001-2009)	68	41.705	12.376
IT-Lav	Lavarone (after 3/2002)	Italy	Evergreen Needleleaf Trees	Bc1	Alpine	12 (2003-2014)	1353	45.956	11.281
IT-MBo	Monte Bondone	Italy	Grasslands	Aa1	Alpine	11 (2003-2013)	1550	46.014	11.045
IT-Noe	Sardinia/ Arca di Noe	Italy	Shrublands	Ad1	Mediterran ea	11 (2004-2014)	25	40.606	8.151
IT-Ren	Renon	Italy	Evergreen Needleleaf Trees	Ac1	Alpine	13 (2001-2013)	1730	46.586	11.433
IT-Ro1	Roccares pampani1	Italy	Deciduous Broadleaf Trees	Da1	Mediterran ea	8 (2001-2008)	235	42.408	11.930
IT-Ro2	Roccares pampani2	Italy	Deciduous Broadleaf Trees	Da1	Mediterran ea	11 (2002-2012)	160	42.390	11.920
IT-SRo	San Rossore	Italy	Evergreen Needleleaf Trees	Cd3	Mediterran ea	12 (2001-2012)	6	43.727	10.284
IT-Tor	Torgnon	Italy	Grassland	Aa1	Alpine	7 (2008-2014)	1260	45.844	7.578
NL-Hor	Horsterm eer	Netherlands	Mixed Trees	Da1	Atlantic	8 (2004-2011)	2	52.240	5.071
NL-Loo	Loobos	Netherlands	Evergreen Needleleaf Trees	Bd2	Atlantic	14 (2001-2014)	25	52.166	5.743

125 **2.2 Satellite-derived Ecosystem Functional Types (EFTs)**

126 To characterize the regional heterogeneity in ecosystem functioning across continental Europe, we identified EFTs based on
127 the 2001-2014 time-series of satellite images of the Enhanced Vegetation Index (EVI) captured by the MODIS-Terra sensor.
128 These images (MOD13Q1.C006 product) provide a maximum composite EVI value every 16 days at a ~230 m spatial
129 resolution. EVI is a proxy for canopy greenness, vegetation carbon gains, or primary production (Huete et al. 1999). Based on
130 the approach by Alcaraz-Segura et al. (2013), we identified EFTs using three biologically meaningful metrics of the EVI
131 seasonal dynamics: the EVI annual mean (EVI_mean; an estimator of annual primary production), the EVI seasonal standard
132 deviation (EVI_SD; a descriptor of seasonality), and the date of maximum EVI (EVI_DMAX; an indicator of phenology). We
133 chose to use MODIS data instead of other satellites with higher spatial resolution (e.g., Landsat or Sentinel-2) because MODIS
134 has several advantages in terms of data availability and quality (e.g. more years of data and cloud-free image every 16-days)
135 along the time series (see S1).

136 The range of values of each EVI metric was divided into four intervals, giving a potential number of 64 EFTs ($4 \times 4 \times 4$). For
137 EVI_DMAX, the four intervals agreed with the four seasons of the year. For EVI_mean and EVI_SD, we extracted the first,
138 second, and third quartiles for each year. For each quartile, we calculated the interannual mean of the 14-year period and used
139 them as breaks between classes. These breaks were applied back to each year as the thresholds for EVI_Mean and EVI_sSD
140 to set EFT classes (S2, Table S1). We used this four-class discretization and fixed class boundaries to obtain a coherent and
141 ecologically interpretable classification (Noble and Gitay 1996) that applies consistently across years. This approach enables
142 interannual comparisons of spatial functional heterogeneity and maintains continuity with previous EFT implementations
143 (Alcaraz-Segura et al. 2013, Cazorla et al. 2021, 2023). Moreover, recent methodological assessments indicate that EFT
144 derivation is robust to the number of bins used to discretize EF attributes (e.g., Liu et al. 2023). To name EFTs, we used two
145 letters and a number: the first capital letter indicates net primary production (EVI_mean), increasing from A to D; the second
146 small letter represents seasonality (EVI_SD), decreasing from a to d; the numbers are a phenological indicator of the growing
147 season (EVI_DMAX), with values 1-spring, 2-summer, 3-autumn, 4-winter (see S3, Table S2 for a schematic summary of
148 code combinations and examples). To summarize the ecosystem functional diversity of the 2001–2014 period, we calculated
149 the dominant EFT (i.e., the mode value for each pixel) of these years.

150 **2.3 Eddy covariance (EC) sites for net ecosystem exchange (NEE)**

151 To obtain NEE fluxes, 50 EC sites were selected across our study area from the FLUXNET2015 dataset (Table 1). The
152 FLUXNET network (Baldocchi et al. 2001, 2020) provides high-quality, community-based, global data on CO₂, H₂O, and
153 energy exchanges between the biosphere and the atmosphere measured using the EC technique (Baldocchi, 2003). We used
154 data of NEE of CO₂ (NEE_VUT_REF, gC m⁻² d⁻¹) from the FLUXNET2015 database. We selected data from
155 FLUXNET2015 because they are publicly available and offer benefits in terms of standardized methodology. FLUXNET2015

156 incorporates NEE measurements along with a quality flag based on an annually determined Variable Ustar Threshold (VUT),
 157 which is selected to maximize model efficiency (MEF) (Pastorello et al. 2020). The MEF analysis is repeated for each one of
 158 the half-hourly data (Baldocchi et al. 2001, 2020). We selected sites that: (a) were located in our study area; (b) provided more
 159 than three consecutive years of data over the 2001-2014 period; (c) provided daily averages of NEE calculated from half-
 160 hourly data; and (d) had quality control information (i.e., NEE_VUT_REF data with quality control flag QC > 1 were removed
 161 since they represent medium and poor quality gap-filled data).

162 We applied Discriminant Analysis (DA) to assess whether different satellite-derived EFT classes correspond to different NEE
 163 dynamics and whether sites under the same EFT exhibit similar NEE dynamics (S4). The DA allowed us to examine the
 164 homogeneity within each EFT class and the differences among EFT classes based on the annual dynamics of NEE as a predictor
 165 variable (Williams,1981, 1983). We selected the EFT where each EC site was located and its corresponding interannual
 166 average of the seasonal cycle of NEE for the available years. EC sites fluxes were regarded as the ground truth standard against
 167 which the satellite data were compared to calculate five performance metrics: Kappa, Accuracy, Precision, Recall, and F1
 168 score (Table 2).

169
 170 **Table 2.** Metrics, interpretations, and equations used to evaluate and compare results from the discriminant analysis, Pr(a) is
 171 the relative observed agreement between observations, and Pr(e) is the hypothetical probability of agreement by chance. True
 172 Positives are correctly classified as positive, True Negative are correctly classified as negative, Positives are all positives
 173 including false positives (i.e., including falsely classified as positive, Type I error) and, Negatives are all negatives including
 174 false negatives (i.e. falsely classified as negative, Type II error). All performance metrics oscillate between 0 (disagreement)
 175 and 1 (maximum agreement).

176

Metric	Meaning	Equation
Kappa	Measures the percentage of data values in the main diagonal of the contingency table and adjusts these values for agreement that could be expected due to chance alone	$K = \frac{\text{Pr}(a) - \text{Pr}(e)}{1 - \text{Pr}(e)}$
Accuracy	Degree of closeness of measurements of a quantity to that quantity's true value	$\text{Accuracy} = \frac{\text{True Positives} + \text{True Negatives}}{\text{Positives} + \text{Negatives}}$

Precision	Fraction of relevant instances among the retrieved instances (also called positive predictive value, i.e., how many EFTs were well discriminated)	$\text{Precision} = \text{True Positives} / (\text{True Positives} + \text{False Positives})$
Recall	Fraction of relevant instances that have been retrieved over the total amount of relevant instances	$\text{Recall} = \text{True Positives} / (\text{True Positives} + \text{False Negatives})$
F1	Considers both the Precision and the Recall of the test to compute the score	$\text{F1 score} = 2 \times (\text{Precision} \times \text{Recall}) / (\text{Precision} + \text{Recall})$

177

178 **2.4 Comparing how EFTs and PFTs discriminate different NEE dynamics**

179 The PFT corresponding to each EC site was assigned by each of their principal investigators using the International Geosphere-
 180 Biosphere Programme (IGBP, 1992). Subsequently, we verified the assigned PFTs using the MODIS MCD12Q1 land cover
 181 product. The PFT categories present in the EC sites were: cropland (15 sites), deciduous broadleaf trees (6), evergreen
 182 needleleaf trees (10), grassland (6), mixed trees (7), shrubland (3), and wetland (1) (Table 1).

183 During the comparison of the performance of PFTs and EFTs to discriminate the seasonal dynamics of NEE, we considered
 184 the unbalanced sample size due to the different number of classes of EFTs (18) and PFTs (7) represented by FLUXNET2015
 185 and the different number of EC sites per PFT class (which ranged between 3 and 31). To do this, we performed the following
 186 steps:

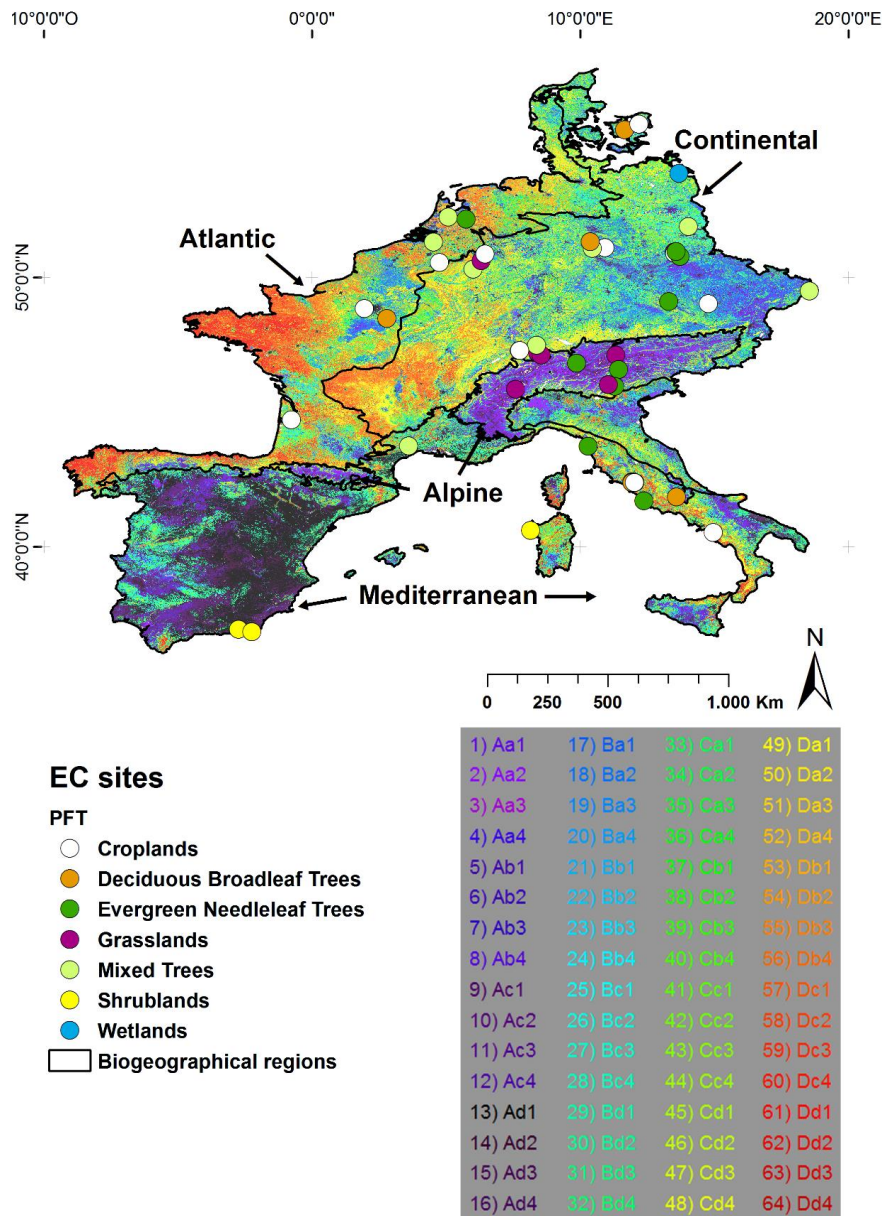
187 First, we calculated all possible combinations (C) without repetitions between the 18 EFT and the 7 PFT classes ($C(18,7) =$
 188 31834). Second, since the DA needs balanced data, we discarded all combinations with different numbers of EC sites in the
 189 combined EFT and PFT classes. Third, for each combination, we applied discriminant analysis to assess how the EFT and PFT
 190 classifications performed to discriminate the seasonal dynamics of NEE. For each discriminant analysis, we obtained five
 191 metrics of performance (Table 2). Fourth, to assess whether significant differences existed in the performance metrics between
 192 EFTs and PFTs, we applied the Wilcoxon non-parametric test. For each combination of a number of classes and EC sites, there
 193 was a different number of discriminant analyses in the EFT subset and the PFT subset (S4 Table S3). To account for such an
 194 unbalanced design during the Wilcoxon test, we fixed the sample size to the smaller subset (either from the EFT or the PFT
 195 classification) and randomly bootstrapped the performance metrics from the bigger one. Fifth, we calculated the mean and
 196 standard deviation of each metric obtained by the EFTs and PFTs classifications, the average p-value, and the percentage of
 197 times we obtained significant differences (p-value <0.05) between EFTs and PFTs.

198 **3 Results**

199 **3.1 Regional heterogeneity in ecosystem functioning using satellite-derived EFTs**

200 The map of the EVI-derived proxies of productivity (EVI_mean), seasonality (EVI_SD), and phenology (DMAX) (S5 Fig.
201 S1a-c) and their integration into EFTs (Fig. 1) provided a characterization of the spatial patterns of our focal ecosystem function
202 across Europe. At the continental scale, productivity decreased eastwards and southwards (Fig. 1, S5 Fig. S4). Seasonality was
203 greater in cultivated and mountain grassland areas (Fig. 1, S5 Fig. S5), and the most frequent EVI maxima occurred in spring
204 and summer (Fig. 1, S5 Fig. S6).

205 The greatest EVI_mean (D) was reached in the Atlantic and Continental biogeographic regions (Fig. 1, S5 Fig. S4d). At the
206 same time, the lowest EVI_mean (A) occurred in the western part of the Mediterranean region, corresponding to most of the
207 Iberian Peninsula, some parts of the Italian Peninsula, the mountainous areas of the Alpine region, and in the eastern part of
208 the Continental region (Fig. 1, S5 Fig. S4a). The greatest seasonality (a) occurred in the highest altitudes of the Alpine region
209 (peaks of Alps <3000 meters), the Continental region (southwestern, northwestern, and eastern part of this region), and the
210 eastern part of the Atlantic region (Fig. 1, S5 Fig. S5a). The lowest seasonality (d) was observed in the western part of the
211 Mediterranean region, specifically in the Iberian Peninsula, the Gulf of Lion's surroundings, and the Atlantic region's Coastal
212 western places (Fig. 1, S5 Fig. S5d). The phenological indicator of the growing season, DMAX, showed that most areas of the
213 Mediterranean region have the EVI maxima in spring (1). EVI maxima in spring (1) were also observed in the Continental and
214 Alpine regions (Fig. 1, S5 Fig. S6a). Maxima in summer (2) were identified in western places of the Atlantic and most of the
215 Alpine regions (Fig. 1, S5 Fig. S6b). EVI maxima in autumn (3) mainly in the Mediterranean region (Fig. 1, S5 Fig. S6c).
216 Maxima in winter (4) were rare and emerged in the eastern part of the Atlantic region, where the maximum productivity was
217 found and in the western part of the Mediterranean region (Fig. 1, S5 Fig. S6d). A simplified representation of the EFT map,
218 obtained by clustering EFTs based on their functional similarity, is provided in the Supplementary Material (S6).



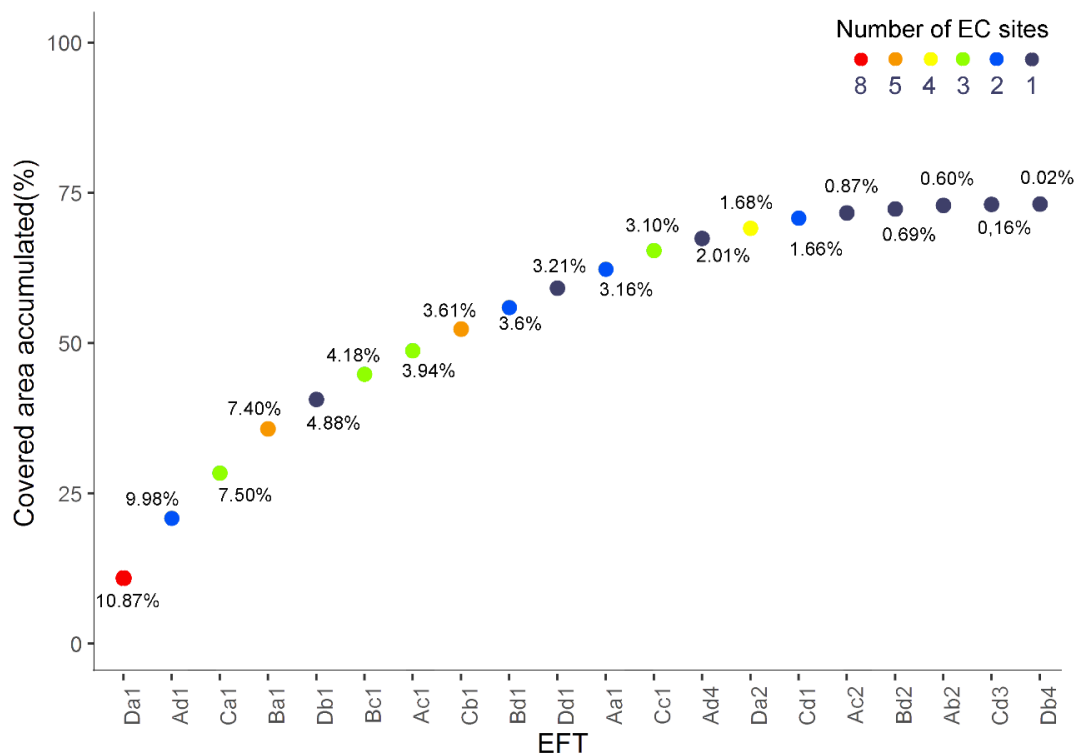
219

220 **Fig. 1.** Ecosystem Functional Types (EFTs) based on MODIS-EVI dynamics (~230 m resolution) and Eddy Covariance (EC)
 221 sites corresponding to the 2001–2014 period. Capital letters in the legend correspond to the EVI annual mean (EVI_mean)
 222 level, ranging from A to D for low to high productivity. Small letters show the seasonal standard deviation (EVI_SD), ranging
 223 from a to d for high to low seasonality of carbon gains. The numbers indicate the season when the maximum EVI took place
 224 (DMAX): (1) spring, (2) summer, (3) autumn, (4) winter. Places with EC sites are indicated with colored circles, where each
 225 color represents a different plant functional type (PFT). Biogeographical regions are based on the official European
 226 biogeographical regions map (EEA, 2016) and are represented by black lines.

227 **3.2 Ground-based NEE of the satellite-derived EFTs**

228 In total, 20 of the 64 potential EFTs, containing 73.10 % of our study area, were represented by the network of the 50 long-
 229 term EC sites that met our selection criteria (Fig. 2). The most abundant EFT, Da1, showed high productivity (D), high
 230 seasonality (a), and maximum EVI in spring (1) (Fig. 2). Da1 occupied 10.87% of the surface and was distributed throughout
 231 the study area but abundantly in the western and southern extremes of the Atlantic Region). Da1 was represented by 8 EC sites
 232 that exhibited NEE with a strong seasonal variability, with a pronounced peak of carbon assimilation between -7.23 and -7.46
 233 g C m⁻² d⁻¹ in spring (Fig. 4) and corresponded with the most abundant ecosystem in Europe, the Deciduous Broadleaf and
 234 Mixed Forest (S4 Table S4). The second most abundant EFT, Ad1, showed low productivity (A), low seasonality (d), and
 235 maximum EVI also in spring (1). Ad1 occupied 9.98% of the territory, mainly in the Iberian Peninsula (Fig. 1). Ad1 was
 236 represented by 2 EC sites (Fig. 2) that exhibited NEE dynamics with low seasonality and the peak of carbon assimilation
 237 (NEE) between -0.72 and -1.98 g C m⁻² d⁻¹ in spring (Fig. 4) and was concentrated in areas dominated by shrub vegetation
 238 (S4 Table S4).

239



240

241 **Fig. 2.** Accumulated area covered by the Ecosystem functional types (EFTs; in %) represented in the study (ordered from
 242 highest to lowest). Colors indicate the number of eddy covariance (EC) sites, and the numbers indicate the area occupied by
 243 each of these EC sites (in %).

244

245 Regarding the abundance of EC sites, the EFT Da1 mentioned above was represented by 8 EC sites, followed by EFT Ba1 and
246 Cb1 with 5 EC sites. The EFT Ba1, was also abundant, occupying 7.4% of the total surface (Fig. 2), and was located mainly
247 in the eastern part of the study area (Atlantic and Continental regions) (Fig. 1). The EFT Cb1, was less abundant than the
248 previous one (3.61%) and was located in central areas of the Atlantic and Continental regions. NEE dynamics were
249 characterized by high (a) and medium-high (b) seasonality and the peak time of carbon assimilation between -6.40 and -7.53
250 g C m⁻² d⁻¹ in spring. In both cases, these places corresponded with cereal crops (S4 Table S4).

251 Our discriminant analysis showed that EFTs significantly differed in NEE measured in situ with the EC technique. The average
252 of the performance metrics obtained from the discrimination that satellite EFTs made of EC site NEE ranged between 0.953
253 to 0.978 (Table 3a). NEE dynamics significantly differed between different EFTs but were similar within the same EFTs (S5
254 Fig. S2). For example, the EFT “Da1”, which had high productivity, high seasonality, and spring EVI maxima, also showed
255 high average NEE values, high seasonality in NEE, and maximum carbon assimilation in spring (Fig. 4, EC sites DE-Lnf, FR-
256 Fon). The EFT “Bc1”, with medium to high productivity, medium seasonality, and spring EVI maxima, was also characterized
257 by moderate seasonality in terms of NEE and maximum carbon assimilation in spring (Fig. 4a for EC sites BE-Vie, DE-Tha).
258 Contrary, the EFT “Ad1”, which had low productivity, low seasonality, and EVI spring maxima, also showed low average
259 NEE, low seasonality in NEE, and a peak of maximum carbon assimilation in spring (ES-Lju, IT-Noe). As another example,
260 the EFT “Cb1”, with medium productivity, medium-high seasonality, and spring EVI maxima, also showed medium to high
261 seasonality in terms of NEE and maximum carbon assimilation in spring (Fig. 4a for EC sites DE-she, DE-RuS).

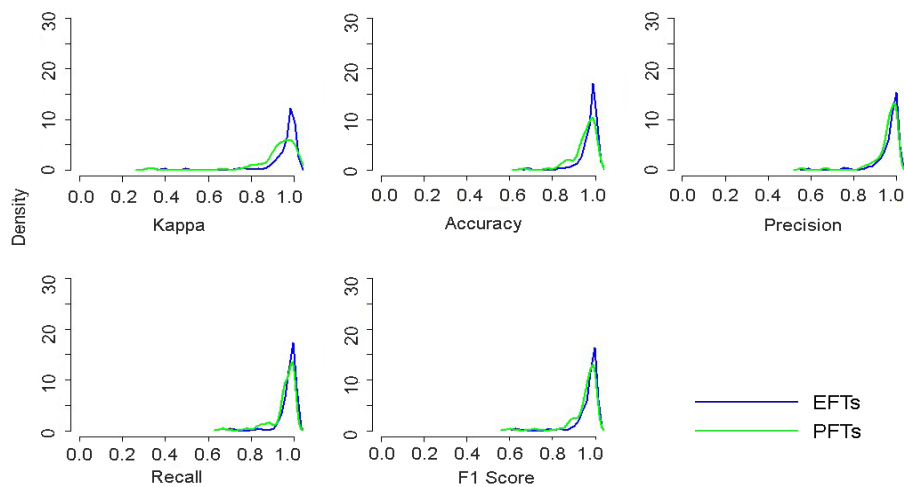
262 3.3 Comparison between EFTs and PFTs to discriminate NEE measured by EC

263 EFTs performed marginally better than PFTs in capturing differences in NEE dynamics measured on the ground (Table 3).
264 The average across all discriminant analyses in all performance indices was marginally but not significantly higher for EFTs
265 (e.g., mean Kappa = 0.953) than for PFTs (e.g., mean Kappa = 0.923) (Table 3, Fig. 3); However, the standard deviation (s.d.)
266 across all discriminant analyses was higher for PFTs (e.g., s. d. of Kappa = 0.078) than for EFTs (e.g., s. d. of Kappa = 0.067).
267 No significant differences between the performance metrics of EFTs and PFTs were detected by the Wilcoxon-test in any of
268 the indices (Table 3).

271 **Table 3.** Mean performances metrics, their standard deviation (SD) and differences in: Kappa, Accuracy, Precision, Recall
272 and F1 values obtained from discriminant analysis of combinations with equal number of classes and EC sites of (a) ecosystem
273 functional types (EFTs) and (b) plant functional types (PFTs). To assess for significant differences, we applied a Wilcoxon-
274 test (p-values showed), and we calculated the percentage of cases in which differences between EFTs or PFTs with NEE were
275 significant (% sig), in this case, none.

276

	a. EFTs		b. PFTs		Difference	
	mean	SD	mean	SD	p-value	% sig
Kappa	0.953	0.067	0.923	0.078	1	0
Accuracy	0.972	0.040	0.952	0.051	1	0
Precision	0.967	0.047	0.959	0.057	1	0
Recall	0.978	0.033	0.960	0.040	1	0
F1	0.972	0.040	0.959	0.048	1	0



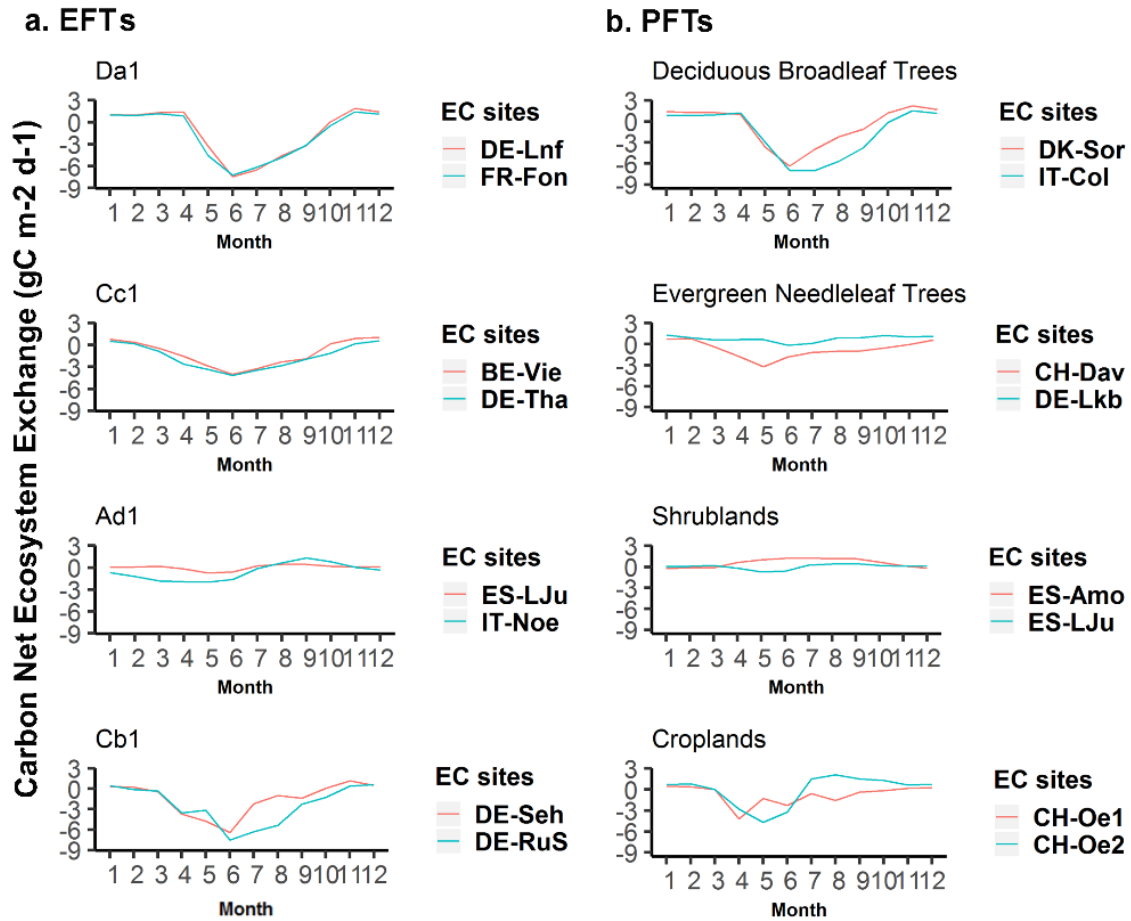
277

278 **Fig. 3.** Histograms of performances from discriminant analysis for all combinations of Ecosystem Functional Types (EFTs)
 279 and Plant Functional Types (PFTs) with equal number of classes and EC sites. Blue lines correspond to EFTs and green lines
 280 to PFTs.

281

282 In general, NEE dynamics were similar for the same PFT or EFT across EC sites (Fig. 4), though there were some exceptions
 283 for certain PFTs (Fig. 4b; S5 Fig. S3). Sites corresponding to the PFT “deciduous broadleaf trees” or the EFT “Da1” always
 284 showed similar NEE (Fig. 4; Table 1). However, for the PFT “evergreen needleleaf trees”, NEE dynamics exhibited a different
 285 seasonality and variable maximum carbon assimilation across sites (Fig. 4b for EC sites CH-Dav, DE-Lkb). Differences in

286 NEE dynamics across sites were also observed for shrublands where the ES-LJu site (EFT Ad1) was assimilating carbon
 287 throughout the year, particularly in spring, while the ES-Amo site (EFT Ad4) was mainly emitting carbon throughout the year
 288 except for winter. Larger differences in NEE occurred in the PFT croplands, with maximum carbon sequestration occurring
 289 in different seasons (Fig. 4b, for sites CH-Oe1 and CH-Oe2 (EFT Cb1)).
 290



291
 292 **Fig. 4.** Comparison of the variability within and across classes of Ecosystem Functional Types (EFTs) and Plant Functional
 293 Types (PFTs) in the seasonal dynamics of NEE. a) Variability inter EFTs: annual mean of NEE dynamics from different places

294 randomly selected with the same EFT; and b) variability inter PFTs and intra EFTs: annual mean of NEE dynamics from
295 different places with the same PFT and different EFT.

296 **4 Discussion**

297 Remotely-sensed EFTs successfully mapped functionally homogeneous land patches regarding NEE dynamics measured in
298 situ with the EC technique. Furthermore, EFTs performed at least similarly to the commonly used PFTs for discriminating
299 among different NEE seasonal dynamics (Table 3). EFTs have the advantage of being more sensitive in their responses to
300 short-term changes in ecosystem functioning than the slower-responding plant community composition or canopy structure.
301 Furthermore, they can be recalculated on an annual basis using the same classification rules, which provides a straightforward
302 way to track interannual changes in ecosystem functioning (Müller et al. 2014). Our focal ecosystem function was NEE
303 dynamics, which is related to primary production (but also to ecosystem respiration), one of the most essential and integrative
304 descriptors of ecosystem functioning (Virginia and Wall, 2010). Hence, satellite-derived EFT classifications could be used to
305 monitor the status and changes of the regional heterogeneity or spatial diversity of the essential variable of ecosystem
306 productivity as a surrogate of the overall ecosystem performance (Jax, 2010; Pettoirelli et al., 2016).

307 **4.1 EFTs capture differences in NEE**

308 EFTs quantified and mapped the spatio-temporal characteristics of carbon dynamics, a crucial aspect for biodiversity
309 conservation and ecosystem services maintenance in a global change context (Midgley et al. 2010). Twenty of the 64 EFTs
310 identified in Europe (corresponding to 73% of the study area) were represented by at least one EC site in the FLUXNET2015
311 dataset with at least three years of data. This number of site-years and the covered area provided sufficient evidence to confirm
312 the validity of the EFT concept. Therefore, our approach could help to assess carbon dynamics at a regional scale by providing
313 homogeneous land areas in terms of their primary production dynamics (Running et al. 2004, Zhang et al. 2015). This fact
314 helps to understand the regional patterns and drivers of the differences in carbon dynamics at the regional scale and could
315 contribute to reducing the uncertainties in the global carbon balance (Beer et al. 2010).

316 EFTs capture spatial differences in NEE seasonal dynamics equally well or marginally better than other mainstream
317 approaches, such as PFTs. Different areas may respond differently to environmental changes despite being dominated by the
318 same PFT, and frequently, ecosystem-process models (parameterized for a specific PFT) may not be able to represent these
319 differential responses (Vargas et al. 2013). Usually, the parameterization of a particular PFT is homogeneous within such PFT
320 and does not change, for instance, according to the eco-physiological status of a specific area or its intrinsic plasticity (Müller
321 et al. 2014). In addition, land-cover maps based on a PFT concept are static and difficult to update (i.e., PFT database structure
322 and assumptions are not easily adapted to new data). At the same time, EFTs are a data-driven classification through which
323 we can annually obtain new data and detect changes in the exchange of matter and energy between the ecosystems and the
324 atmosphere in response to environmental variability. In this sense, the literature (Bret-Harte et al. 2008; Suding et al. 2008;

325 Clark et al. 2016; Saccone and Virtanen 2017; Thomas et al. 2018) has pointed out that the PFT approach is not straightforward
326 enough to represent ecosystem functional properties at the ecosystem level.

327 EFTs derived in this study rely on EVI-based attributes, which primarily represent the dynamics of primary production. This
328 focus is consistent with the fact that vegetation greenness and light absorption are tightly linked to APAR, GPP and NEE (e.g.
329 Huete et al. 1997; Running et al. 2004; Shi et al. 2017), making EVI a direct and widely used indicator of ecosystem functional
330 behaviour at large scales. The strong agreement between our EFTs and in situ NEE patterns confirms that EVI captures the
331 dominant functional axis related to carbon uptake. Although additional attributes associated with water or energy fluxes (e.g.,
332 NDWI, land-surface temperature or albedo) could enrich multidimensional EFT frameworks in the future, the carbon-related
333 dynamics encoded in EVI already provide a robust and ecologically meaningful foundation for functional ecosystem
334 classification.

335 **4.2 EFT spatial patterns and environmental controls**

336 EFTs allowed us to characterize the regional heterogeneity of ecosystem functioning across Europe. In relation to the three
337 descriptive attributes of ecosystem functioning from which the EFTs were constructed (EVI_mean; an estimator of primary
338 production, EVI_SD; a descriptor of seasonality and EVI_DMAX; an indicator of phenology), we found general patterns
339 determined by the combination of vegetation characteristics and environmental controls. The role of environmental variables
340 (abiotic and biotic) that control ecosystem processes differ according to the level of biological organization and the spatial
341 scale considered (Reed et al. 1993; Pearson and Dawson, 2003). Ecosystem functioning in natural areas are known to be mainly
342 driven by precipitation (Lauenroth et al. 1978), temperature (Rosenzweig and Dickinson 1968; Jobbagy et al. 2002), soil
343 characteristics (NoyMeir 1973), and vegetation structure (Epstein et al. 1998). In this case, EFTs productivity decreased from
344 east to west influenced by rainfall patterns determined by the Gulf Stream and the distance from the ocean (Palter 2015), which
345 also determines changes in vegetation. Regarding the seasonality of EVI, it increased in relation to two factors: 1) the altitude,
346 having the highest values of seasonality in the mountainous areas (influenced by changes in precipitation, temperature, and
347 consequently, in vegetation), and; 2) the crop areas, where management practices, harvests, and crop changes are responsible
348 of this dynamic and therefore it cannot be explained by natural environmental controls alone. Peaks of maximum EVI in
349 Europe took place in spring and summer when the availability of water (precipitation) and energy (temperature) for vegetation
350 was at its optimum (Whittaker et al. 2003).

351 Boundaries of the biogeographical regions (EEA 2016) were consistent with the EFTs (Fig. 1). Still, while the classification
352 from EEA is static, EFTs provide a data-driven classification that could be better coupled to ecosystem functioning. The Alpine
353 region was dominated by EFTs with low productivity, high seasonality, and maxima in summer. In the high mountain peaks
354 (<3000 meters), the vegetation was reduced to a low density of highly adapted plants that can tolerate extreme conditions (i.e.,
355 the short growing period and fluctuating air temperatures, and therefore, has low productivity, also detected in the global
356 primary productivity patterns of Beer et al. (2010) and Zhang et al. (2017)). In the highest altitudes, snow is present over most

357 of the year, leaving only a short period for the development of the plants, mainly in summer, leading to a summer maximum
358 and a high seasonality (Sundseth, 2009a).

359 A high heterogeneity of EFTs characterized the Mediterranean region due to their high habitat diversity (i.e., high mountains
360 and rocky shores, thick scrub and semi-arid steppes, coastal wetlands, and sandy beaches, constituting a global biodiversity
361 hotspot (Myers et al. 2000)). The main driver of ecosystem functional diversity is the climate (characterized by hot, dry
362 summers and cool winters) (Lionello et al. 2006), in combination with human influence, (i.e., livestock grazing, forest
363 cultivation, and forest fires) (Blondel and Aronson, 1999).

364 The Atlantic region was characterized by EFTs with high productivity, high seasonality, and maximum greening in spring due
365 to the mild winters, cool summers, predominantly westerly winds, and moderate rainfall throughout the year (Hurrel, 1995).
366 These conditions favor non-water-limited deciduous species with high productivity, resulting in a high seasonality. Due to the
367 anthropogenic influence, agricultural landscapes are widespread in this region, one of Europe's five major agricultural regions,
368 according to Kostrowicki (1991). Thus, the region's high productivity must be partly attributed to irrigation, and high
369 seasonality is driven by harvest and cropping cycles.

370 Finally, in the Continental region, the ecosystem's functioning varied largely in terms of productivity, reflecting regional
371 climatic patterns. In the eastern part of the continental region, extremes of hot and cold temperatures and wet and dry conditions
372 are more frequent and strongly impact ecosystem functioning (dominant EFT was Aa1, low productivity, high seasonality, and
373 maximum in spring). These areas are mountainous and experience sub-alpine conditions. Moving west, the climate is
374 characterized by relatively small temperature fluctuations due to the buffering effect of the nearby ocean and the flat landscape
375 (Da1 and Ca1 in the transition) (Sundseth, 2009b).

376 **4.3 Opportunities and limitations of EFTs**

377 Since EFTs describe ecosystem functioning on an annual basis in homogeneous patches on the land surface, they offer
378 opportunities for application in ecology and conservation compared to approaches that do not represent short-term dynamics
379 (such as PFTs). The concept of EFT has been highlighted as “the first serious attempt to group ecosystems (at large scales)
380 based on shared functional behavior” (Mucina, 2019), and its strength for being applied as a classification scheme is determined
381 by its ability to translate ecosystem functions into discrete entities that can be mapped. EFTs are identified by remote sensing
382 tools from aggregated measurements of ecosystem functions at the pixel level, which, in practice, represents information on
383 the performance of the whole ecosystem at that grain scale. Having the possibility of mapping entities (EFTs) that reflect the
384 principal performance of the entire ecosystem opens a straightforward, tangible, and biologically meaningful way to quantify
385 distributions of ecosystem functions at the regional scale, complementing our traditional view of ecosystems (Paruelo et al.
386 2001; Butchart et al. 2010; Asner et al. 2017). Specifically, satellite-derived dynamic functional classifications, such as EFTs,
387 have several advantages over other static approaches, such as PFTs. Satellite-derived EFAs and EFTs 1) are capable of
388 capturing differences in ecosystem processes as measured in the field; 2) they provide a valuable framework for understanding
389 the mechanisms underlying large-scale ecological changes (Cabello et al. 2016; Alcaraz-Segura et al. 2017; Requena-Mullor

390 et al. 2017, 2018; Arenas-Castro et al. 2018; Lourenço et al. 2018; Vaz et al. 2018); 3) they offer a faster response than
391 compositional or structural approaches to environmental changes (McNaughton, 1989; Mouillot et al. 2013), which are
392 particularly noticeable at the ecosystem level (Vitousek, 1994); 4) they can be more easily monitored and updated than
393 structural or compositional ones under a common protocol in space and time, at different spatial scales and over large
394 extents (Paruelo et al. 2001); 5) they can complement information on vegetation structure and composition (e.g., canopy
395 architecture, vegetation type, PFT), because they constitute complementary dimensions of biodiversity complexity (Noss,
396 1990); 6) they facilitate the direct assessment of ecosystem functions and services (Costanza et al. 2006; Hellmann et al. 2017)
397 and would link critical dimensions of biodiversity to ecosystem processes including the carbon cycle, the water cycle and the
398 provisioning of ecosystem services; 7) they have already been proposed as essential variables for monitoring biodiversity
399 (Pettorelli et al. 2016; Skidmore et al. 2021).

400 Our approach, as with any other ecosystem classification framework, is still subject to some challenges. First, EFTs represented
401 by several EC sites could be parameterized in terms of NEE dynamics, though not all EFTs (18%) are represented yet.
402 Nevertheless, the subset of EFTs covered by multiple EC sites spans the dominant functional types across Europe, providing
403 a solid empirical basis for validating the classification. Second, the footprint or spatial resolution of the EC measurements
404 varies depending on the micrometeorological conditions (wind direction, wind speed, atmospheric stability) and the ratio of
405 measurement to vegetation height, e.g., forest flux footprints are generally larger than grassland footprints (oscillates between
406 50 m and 200 m) (Schmid 1997; Kljun et al. 2015). In contrast, the MODIS pixels used have a constant spatial resolution of
407 ~231 m, generating an unavoidable scale mismatch. However, because EC towers are typically placed in relatively large and
408 functionally homogeneous land patches (Aubinet et al. 2012), the MODIS pixel and the flux footprint generally sample
409 comparable surfaces, limiting the practical impact of this mismatch on the regional-scale patterns captured by our EFTs.
410 Nonetheless, we acknowledge that some challenges regarding spatial representativeness remain (Chu et al. 2021). Future
411 studies may reduce this mismatch by using higher-resolution sensors such as Sentinel-2 (10 m/pixel), but currently is not
412 possible because the time period of Sentinel-2 data is not covered by FLUXNET data (i.e., Sentinel-2 starts taking data in 2015
413 and the available FLUXNET 2015 database goes up to this year). Alternatively, footprint modelling could be applied when
414 appropriate micrometeorological data exist, but footprint-weighted averaging was not feasible in our study because daily or
415 sub-daily footprint estimates are unavailable for most FLUXNET sites and years, a limitation commonly acknowledged in
416 previous RS-flux integration studies (Chu et al. 2021). Third, different ecosystems regarding other functional aspects (e.g.,
417 evapotranspiration, heat exchange) can be classified here as the same EFT from the NEE dynamics, as we used it as our
418 focal function. However, EFTs could also be identified to characterize the spatiotemporal heterogeneity of multiple ecosystem
419 processes and functions at different scales, including other functional aspects (e.g., albedo, evapotranspiration, heat exchange)
420 (Fernandez et al. 2010). Also other temporal metrics, such as daily anomalies or interannual variability can provide
421 complementary information on short-term or year-to-year ecosystem responses, but they are not expected to improve the
422 discrimination among EFTs, which is intrinsically based on intra-annual functional patterns. Similarly, additional phenological
423 transition metrics such as the start and end of the season (SOS/EOS) may offer complementary insights into growing-season

424 timing and duration; however, their higher sensitivity to noise and temporal gaps, particularly in 16-day MODIS time series,
425 makes peak-greenness metrics like EVI_DMAX more robust and comparable for regional-scale functional classifications.
426 Finally, incorporating EFTs into earth system models is challenging since these models generally use simple and few numbers
427 of categories in a variable, and some models might not be able to run with so many (64) EFT categories. Nevertheless, some
428 studies have successfully incorporated EFTs into earth system models (Lee et al. 2013; Müller et al. 2014). The incorporation
429 of these types of variables (dynamic and easily accessible) into the models might be helpful in the monitoring and sustainable
430 management of carbon reservoirs at short to medium-time scales.

431 **5 Conclusion**

432 Satellite-derived EFTs are an ecosystem functional classification built from satellite observations of radiation exchanges
433 between the land surface and the atmosphere that allow the identification of homogeneous land patches in terms of an essential
434 ecosystem function, e.g., NEE dynamics, measured on the ground by means of which is related to ecosystem productivity.
435 EFTs performed as well as PFTs in discriminating different NEE dynamics, EFTs, however, have two main advantages: they
436 can be easily updated for any region of the world at an annual frequency based on available satellite information, and EFTs
437 maps are more sensitive to environmental changes than vegetation composition or structure.

438 Our results showed the capability of using ecosystem functional attributes for grouping ecosystems at large scales according
439 to their different net carbon flux dynamics. Such classification, based on the essential biodiversity variable of ecosystem
440 production as a focal ecosystem function, opens the possibility of assessing and monitoring ecosystem functional diversity,
441 the spatial heterogeneity in ecosystem functioning, and carbon-related ecosystem services at regional to global scales.
442 Therefore, our study demonstrates that satellite-derived EFTs provide a valid tool to assess and monitor ecosystem functioning
443 with potential applications in ecosystem monitoring and modeling and biodiversity and carbon management programs.

445 **Data availability**

446 The MODIS database used in this work is maintained by NASA (satellite Terra, sensor MODIS, product MOD13Q1.006) and
447 is mirrored by Google on the Earth Engine servers ([https://developers.google.com/earth-
448 engine/datasets/catalog/MODIS_006_MOD13Q1](https://developers.google.com/earth-engine/datasets/catalog/MODIS_006_MOD13Q1)). FLUXNET2015 eddy covariance data are available through the
449 FLUXNET website (<https://fluxnet.org/data/fluxnet2015-dataset>). The Google Earth Engine code used to derive Ecosystem
450 Functional Types (EFTs) is openly available at <https://doi.org/10.5281/zenodo.7524973>. [The Ecosystem Functional Types
451 \(EFTs\) map generated in this study is available on Zenodo at https://zenodo.org/records/18325891](https://zenodo.org/records/18325891). The plant functional types
452 (PFTs) used in this study are based on the IGBP-DIS global 1 km land cover data set "DISCover": proposal and implementation
453 plans, IGBP-DIS available at https://daac.ornl.gov/ISLSCP_II/guides/edc_landcover_xdeg.html.

454

455

456 **Author contributions**

457 DAS, AM, JC, JP and BPC designed the study, AM and DAS coordinated it. BPC processed the data and prepared the
458 manuscript with contributions from all authors. BPC and JML prepared the final Fig.s. LM, AK, LS, BG, JD, LŠ, AI, GW,
459 EP, KF, AM, MP, LM, LH, PD, IG, and KP provided FLUXNET data. All authors reviewed the article and provided valuable
460 feedback, especially RV and JML.

461

462 **Competing interests.** Some authors are members of the editorial board of journal Biogeosciences.

463 **Acknowledgements.** This publication is part of the EVEREST project (PID2023-151939OB-I00) funded by
464 MICIU/AEI/10.13039/501100011033 and by ERDF/EU. Funds were also provided by ERDF and Spanish MINECO (project
465 CGL2014-61610-EXP). This research was also supported by the project “Earth observations for the characterisation and
466 monitoring of ecosystem functioning in Sierra Nevada (Spain)” (C-EXP-074-UGR23), which has been co-funded by the 2014-
467 2020 FEDER Program and the Consejería de Economía, Conocimiento, Empresas y Universidad of the Andalusian
468 Government; ECOPOTENTIAL, which received funding from the European Union’s Horizon 2020 Research and Innovation
469 Program under grant agreement No. 641762, and the NASA 2016 GEOBON Work Programme Grant # 80NSSC18K0446.
470 EarthCul (reference PID2020-118041GB-I00), funded by the Spanish Ministry of Science and Innovation, Smart-
471 EcoMountains, LifeWatch-ERIC action line, within the Workpackages LifeWatch-2019-10-UGR-01_WP-8, LifeWatch-2019-
472 10-UGR-01_WP-7, and LifeWatch-2019-10-UGR-01_WP-4. Additional support was provided by the “Plan Complementario
473 de I+D+i en Biodiversidad (PCBIO)” through the covery Plan - NextGenerationEU, the Spanish Ministry of Science, and the
474 Regional Government of Andalusia (PID2022-140092OB-I00, MCIN/AEI/FEDER, UE). This work used eddy covariance
475 data acquired and shared by the FLUXNET community. The ERA-Interim reanalysis data are provided by ECMWF and
476 processed by LSCE. The FLUXNET eddy covariance data processing and harmonization was carried out by the European
477 Fluxes Database Cluster, AmeriFlux Management Project, and Fluxdata project of FLUXNET, with the support of CDIAC
478 and ICOS Ecosystem Thematic Center, and the OzFlux, ChinaFlux and AsiaFlux offices. JML was funded by the Plan Propio
479 de Investigación (P9) of the University of Granada. AM was supported by the Deutsche Forschungsgemeinschaft (DFG,
480 German Research Foundation) under Germany’s Excellence Strategy – EXC 2070 – 390732324. LM acknowledges the
481 funding provided by Forest Services, Autonomous Province of Bolzano. LŠ acknowledges support from the Ministry of
482 Education, Youth and Sports of the Czech Republic within the CzeCOS program (grant number LM2023048) and the AdAgriF
483 project (CZ.02.01.01/00/22 008/0004635).

484

485 **References**

- 486 Alcaraz, D., Paruelo, J., and Cabello, J.: Identification of current ecosystem functional types in the Iberian Peninsula, *Glob.*
487 *Ecol. Biogeogr.*, 15, 200–212, <https://doi.org/10.1111/j.1466-822X.2006.00215.x>, 2006.
- 488 Alcaraz-Segura, D., Paruelo, J. M., Epstein, H. E., and Cabello, J.: Environmental and human controls of ecosystem
489 functional diversity in temperate South America, *Remote Sens.*, 5, 127–154, <https://doi.org/10.3390/rs5010127>, 2013.
- 490 Arenas-Castro, S., Gonçalves, J., Alves, P., Alcaraz-Segura, D., and Honrado, J. P.: Assessing the multi-scale predictive
491 ability of ecosystem functional attributes for species distribution modelling, *PLoS ONE*, 13, e0199292,
492 <https://doi.org/10.1371/journal.pone.0199292>, 2018.
- 493 Armstrong, A., Alcaraz-Segura, D., Reynolds, M., and Epstein, H.: Ecosystem functional types of the circumpolar Arctic
494 tundra based on the seasonal dynamics of vegetation productivity, *Environ. Res. Ecol.*, 3, 025003,
495 <https://doi.org/10.1088/2752-664X/ad4beb>, 2024.
- 496 Arenas-Castro, S., Regos, A., Gonçalves, J. F., Alcaraz-Segura, D., and Honrado, J.: Remotely sensed variables of
497 ecosystem functioning support robust predictions of abundance patterns for rare species, *Remote Sens.*, 11, 2086,
498 <https://doi.org/10.3390/rs11182086>, 2019.
- 499 Asner, G. P., Martin, R. E., Knapp, D. E., Tupayachi, R., Anderson, C. B., Sinca, F., Vaughn, N. R., and Llactayo, W.:
500 Airborne laser-guided imaging spectroscopy to map forest trait diversity and guide conservation, *Science*, 355, 385–389,
501 <https://doi.org/10.1126/science.aaj1987>, 2017.
- 502 Baldocchi, D. D.: Assessing the eddy covariance technique for evaluating carbon dioxide exchange rates of ecosystems: past,
503 present and future, *Glob. Change Biol.*, 9, 479–492, <https://doi.org/10.1046/j.1365-2486.2003.00629.x>, 2003.
- 504 Baldocchi, D. D.: How eddy covariance flux measurements have contributed to our understanding of Global Change
505 Biology, *Glob. Change Biol.*, 26, 242–260, <https://doi.org/10.1111/gcb.14807>, 2020.
- 506 Baldocchi, D., Falge, E., Gu, L., Olson, R., Hollinger, D., Running, S., Anthoni, P., Bernhofer, C., Davis, K., Evans, R., et
507 al.: FLUXNET: A new tool to study the temporal and spatial variability of ecosystem-scale carbon dioxide, water vapor, and
508 energy flux densities, *Bull. Am. Meteorol. Soc.*, 82, 2415–2434, [https://doi.org/10.1175/1520-0477\(2001\)082<2415:FANTTS>2.3.CO;2](https://doi.org/10.1175/1520-0477(2001)082<2415:FANTTS>2.3.CO;2), 2001.
- 510 Balvanera, P., Quijas, S., Karp, D. S., Ash, N., Bennett, E. M., Boumans, R., et al.: Ecosystem services, in: *The GEO*
511 *Handbook on Biodiversity Observation Networks*, edited by: Walters, M. and Scholes, R. J., Springer, 39–78,
512 https://doi.org/10.1007/978-3-319-27288-7_3, 2017.
- 513 Beer, C., Reichstein, M., Tomelleri, E., Ciais, P., Jung, M., Carvalhais, N., et al.: Terrestrial gross carbon dioxide uptake:
514 global distribution and covariation with climate, *Science*, 329, 834–838, <https://doi.org/10.1126/science.1184984>, 2010.
- 515 Blondel, J. and Aronson, J.: *Biology and Wildlife of the Mediterranean Region*, Oxford University Press, Oxford, 328 pp.,
516 1999.
- 517 Bret-Harte, M. S., Mack, M. C., Goldsmith, G. R., Sloan, D. B., DeMarco, J., Shaver, G. R., et al.: Plant functional types do

518 not predict biomass responses to removal and fertilization in Alaskan tussock tundra, *J. Ecol.*, 96, 713–726,
519 <https://doi.org/10.1111/j.1365-2745.2008.01378.x>, 2008.

520 Butchart, S. H. M., Walpole, M., Collen, B., van Strien, A., Scharlemann, J. P. W., Almond, R. E. A., et al.: Global
521 biodiversity: indicators of recent declines, *Science*, 328, 1164–1168, <https://doi.org/10.1126/science.1187512>, 2010.

522 Cabello, J., Alcaraz-Segura, D., Reyes, A., Lourenço, P., Requena, J. M., Bonache, J., et al.: System for monitoring
523 ecosystem functioning of Network of National Parks of Spain with remote sensing, *Rev. Teledetección*, 46, 119,
524 <https://doi.org/10.4995/raet.2016.4122>, 2016.

525 Cabello, J., Fernández, N., Alcaraz-Segura, D., Oyonarte, C., Piñeiro, G., Altesor, A., et al.: The ecosystem functioning
526 dimension in conservation: insights from remote sensing, *Biodivers. Conserv.*, 21, 3287–3305,
527 <https://doi.org/10.1007/s10531-012-0370-7>, 2012.

528 Cazorla, B., Cabello, J., Peñas, J., Garcillán, P. P., Reyes, A., and Alcaraz-Segura, D.: Incorporating ecosystem functional
529 diversity into geographic conservation priorities using remotely-sensed Ecosystem Functional Types, *Ecosystems*,
530 <https://doi.org/10.1007/s10021-020-00497-3>, 2020.

531 Cazorla, B., Cabello, J., Reyes, A., Guirado, E., Peñas, J., Pérez-Luque, A. J., and Alcaraz-Segura, D.: A remote-sensing-
532 based dataset to characterize the ecosystem functioning and functional diversity in the Biosphere Reserve of the Sierra
533 Nevada (southeastern Spain), *Earth Syst. Sci. Data*, 15, 1871–1887, <https://doi.org/10.5194/essd-15-1871-2023>, 2023.

534 Cazorla, B., Garcillán, P. P., Cabello, J., Alcaraz-Segura, D., Reyes, A., and Peñas, J.: Patterns of ecosystem functioning as
535 tool for biological regionalization: the case of the mediterranean-desert-tropical transition of Baja California, *Mediterr. Bot.*,
536 42, e68529, <https://doi.org/10.5209/mbot.68529>, 2021.

537 Chu, H., Luo, X., Ouyang, Z., Chan, W. S., Dengel, S., Biraud, S. C., et al.: Representativeness of eddy-covariance flux
538 footprints for areas surrounding AmeriFlux sites, *Agric. For. Meteorol.*, 301, 108350,
539 <https://doi.org/10.1016/j.agrformet.2021.108350>, 2021.

540 Clark, J. S.: Why species tell more about traits than traits about species: predictive analysis, *Ecology*, 97, 1979–1993,
541 <https://doi.org/10.1002/ecy.1453>, 2016.

542 Costanza, R., d’Arge, R., de Groot, R., Farber, S., Grasso, M., Hannon, B., et al.: The value of the world’s ecosystem
543 services and natural capital, *Nature*, 387, 253–260, <https://doi.org/10.1038/387253a0>, 1997.

544 Costanza, R., Wilson, M., Troy, A., Voinov, A., Liu, S., and D’Agostino, J.: The value of New Jersey’s ecosystem services
545 and natural capital, Institute for Sustainable Solutions, Burlington, VT, 2006.

546 Díaz, S., Purvis, A., Cornelissen, J. H. C., Mace, G. M., Donoghue, M. J., Ewers, R. M., et al.: Functional traits, the
547 phylogeny of function, and ecosystem service vulnerability, *Ecol. Evol.*, 3, 2958–2975, <https://doi.org/10.1002/ece3.601>,
548 2013.

549 Díaz, S., Settele, J., Brondízio, E., Ngo, H., Guèze, M., Agard, J., et al.: Summary for policymakers of the global assessment
550 report on biodiversity and ecosystem services of IPBES, IPBES Secretariat, Bonn, 2020.

551 Domingo-Marimon, C., Jenerowicz-Sanikowska, M., Pesquer, L., Ruciński, M., Krupiński, M., Woźniak, E., et al.:
552 Developing an early warning land degradation indicator based on geostatistical analysis of Ecosystem Functional Types
553 dynamics, *Ecol. Indic.*, 169, 112815, <https://doi.org/10.1016/j.ecolind.2023.112815>, 2024.

554 Epstein, H. E., Burke, I. C., and Mosier, A. R.: Plant effects on spatial and temporal patterns of nitrogen cycling in shortgrass
555 steppe, *Ecosystems*, 1, 374–385, <https://doi.org/10.1007/s100219900030>, 1998.

556 European Environment Agency: Biogeographical regions dataset, [https://www.eea.europa.eu/data-and-](https://www.eea.europa.eu/data-and-maps/data/biogeographical-regions-europe-3)
557 [maps/data/biogeographical-regions-europe-3](https://www.eea.europa.eu/data-and-maps/data/biogeographical-regions-europe-3), 2016.

558 Fernández, N., Paruelo, J. M., and Delibes, M.: Ecosystem functioning of protected and altered Mediterranean environments:
559 a remote sensing classification in Doñana, Spain, *Remote Sens. Environ.*, 114, 211–220,
560 <https://doi.org/10.1016/j.rse.2009.09.009>, 2010.

561 Franz, D., Acosta, M., Altimir, N., Arriga, N., Arrouays, D., Aubinet, M., et al.: Towards long-term standardised carbon and
562 greenhouse gas observations for monitoring Europe’s terrestrial ecosystems: a review, *Int. Agrophys.*, preprint,
563 <https://doi.org/10.2134/agronj2018.02.0114>, 2018.

564 Funk, J. L., Larson, J. E., Ames, G. M., Butterfield, B. J., Cavender-Bares, J., Firn, J., et al.: Revisiting the holy grail: using
565 plant functional traits to understand ecological processes, *Biol. Rev.*, 92, 1156–1173, <https://doi.org/10.1111/brv.12275>,
566 2017.

567 Gomasasca, U., Duveiller, G., Pacheco-Labrador, J., Ceccherini, G., Cescatti, A., Girardello, M., et al.: Satellite remote
568 sensing reveals the footprint of biodiversity on multiple ecosystem functions across the NEON eddy covariance network,
569 *Environ. Res. Ecol.*, 3, 045003, <https://doi.org/10.1088/2752-664X/ad54fb>, 2024.

570 Hellmann, C., Große-Stoltenberg, A., Thiele, J., Oldeland, J., and Werner, C.: Heterogeneous environments shape invader
571 impacts: integrating environmental, structural and functional effects by isoscapes and remote sensing, *Sci. Rep.*, 7, 4118,
572 <https://doi.org/10.1038/s41598-017-04480-w>, 2017.

573 Huang, X., Xiao, J., and Ma, M.: Evaluating the performance of satellite-derived vegetation indices for estimating gross
574 primary productivity using FLUXNET observations across the globe, *Remote Sens.*, 11, 1823,
575 <https://doi.org/10.3390/rs11151823>, 2019.

576 Hurrell, A.: *The Global Environment*, in: *International Relations Theory Today*, Polity Press, Cambridge, UK, 1995.

577 IGBP: The IGBP-DIS global 1 km land cover data set "DISCover": proposal and implementation plans, report of the Land
578 Cover Working Group of IGBP-DIS, IGBP-DIS Office, Toulouse, France, 1992.

579 Ivits, E., Cherlet, M., Mehl, W., and Sommer, S.: Ecosystem functional units characterized by satellite observed phenology
580 and productivity gradients: a case study for Europe, *Ecol. Indic.*, 27, 17–28, <https://doi.org/10.1016/j.ecolind.2012.11.011>,
581 2013.

582 Jax, K.: *Ecosystem Functioning*, Cambridge University Press, Cambridge, UK, 280 pp.,
583 <https://doi.org/10.1017/CBO9780511781216>, 2010.

584 Jetz, W., McGeoch, M. A., Guralnick, R., Ferrier, S., Beck, J., Costello, M. J., et al.: Essential biodiversity variables for

585 mapping and monitoring species populations, *Nat. Ecol. Evol.*, 3, 539–551, <https://doi.org/10.1038/s41559-019-0826-1>,
586 2019.

587 Jobbágy, E. G., Sala, O. E., and Paruelo, J. M.: Patterns and controls of primary production in the Patagonian steppe: a
588 remote sensing approach, *Ecology*, 83, 307–319, [https://doi.org/10.1890/0012-9658\(2002\)083\[0307:PACOPP\]2.0.CO;2](https://doi.org/10.1890/0012-9658(2002)083[0307:PACOPP]2.0.CO;2),
589 2002.

590 Jung, M., Schwalm, C., Migliavacca, M., Walther, S., Camps-Valls, G., Koirala, S., et al.: Scaling carbon fluxes from eddy
591 covariance sites to globe: synthesis and evaluation of the FLUXCOM approach, *Biogeosciences*, 17, 1343–1365,
592 <https://doi.org/10.5194/bg-17-1343-2020>, 2020.

593 Knox, S. H., Jackson, R. B., Poulter, B., McNicol, G., Fluet-Chouinard, E., Zhang, Z., et al.: FLUXNET-CH₄ synthesis
594 activity: objectives, observations, and future directions, *Bull. Am. Meteorol. Soc.*, 100, 2607–2632,
595 <https://doi.org/10.1175/BAMS-D-18-0268.1>, 2019.

596 Kostrowicki, J.: Trends in the transformation of European agriculture, in: *Land Use Changes in Europe*, edited by: Brouwer,
597 F. M., Thomas, A. J., and Chadwick, M. J., Springer Netherlands, Dordrecht, 21–47, https://doi.org/10.1007/978-94-011-3060-5_3, 1991.

599 Lauenroth, W. K., Dodd, J. L., and Sims, P. L.: The effects of water- and nitrogen-induced stresses on plant community
600 structure in a semiarid grassland, *Oecologia*, 36, 211–222, <https://doi.org/10.1007/BF00349815>, 1978.

601 Lavorel, S. and Garnier, E.: Predicting changes in community composition and ecosystem functioning from plant traits:
602 revisiting the Holy Grail, *Funct. Ecol.*, 16, 545–556, <https://doi.org/10.1046/j.1365-2435.2002.00664.x>, 2002.

603 Lavorel, S., Díaz, S., Cornelissen, J. H. C., Garnier, E., Harrison, S. P., McIntyre, S., et al.: Plant functional types: are we
604 getting any closer to the Holy Grail?, in: *Terrestrial Ecosystems in a Changing World*, edited by: Canadell, J. G., Pataki, D.
605 E., and Pitelka, L. F., Springer, Berlin, Heidelberg, 149–164, https://doi.org/10.1007/978-3-540-32730-1_13, 2007.

606 Lee, S.-J., Berbery, E. H., and Alcaraz-Segura, D.: The impact of ecosystem functional type changes on the La Plata Basin
607 climate, *Adv. Atmos. Sci.*, 30, 1387–1405, <https://doi.org/10.1007/s00376-012-2071-y>, 2013.

608 Lionello, P., Malanotte-Rizzoli, P., Boscolo, R., Alpert, P., Artale, V., Li, L., et al.: The Mediterranean climate: an overview
609 of the main characteristics and issues, in: *Developments in Earth and Environmental Sciences*, vol. 4, edited by: Lionello, P.,
610 Malanotte-Rizzoli, P., and Boscolo, R., Elsevier, Amsterdam, 1–26, [https://doi.org/10.1016/S1571-9197\(06\)80003-0](https://doi.org/10.1016/S1571-9197(06)80003-0), 2006.

611 Liu, L., Smith, J. R., Armstrong, A. H., Alcaraz-Segura, D., Epstein, H. E., Echeverri, A., et al.: Influences of satellite sensor
612 and scale on derivation of ecosystem functional types and diversity, *Remote Sens.*, 15, 5593,
613 <https://doi.org/10.3390/rs15235593>, 2023.

614 Liu, Y., Wu, C., Wang, X., and Zhang, Y.: Contrasting responses of peak vegetation growth to asymmetric warming:
615 evidences from FLUXNET and satellite observations, *Glob. Change Biol.*, 29, 2363–2379,
616 <https://doi.org/10.1111/gcb.16624>, 2023.

617 Lourenço, P., Alcaraz-Segura, D., Reyes-Díez, A., Requena-Mullor, J. M., and Cabello, J.: Trends in vegetation greenness
618 dynamics in protected areas across borders: what are the environmental controls?, *Int. J. Remote Sens.*, 39, 4699–4713,

619 <https://doi.org/10.1080/01431161.2018.1448485>, 2018.

620 Malaterre, C., Dussault, A. C., Rousseau-Mermans, S., Barker, G., Beisner, B. E., Bouchard, F., et al.: Functional diversity:
621 an epistemic roadmap, *BioScience*, 69, 800–811, <https://doi.org/10.1093/biosci/biz086>, 2019.

622 McNaughton, S. J., Oesterheld, M., Frank, D. A., and Williams, K. J.: Ecosystem-level patterns of primary productivity and
623 herbivory in terrestrial habitats, *Nature*, 341, 142–144, <https://doi.org/10.1038/341142a0>, 1989.

624 Midgley, G. F., Bond, W. J., Kapos, V., Ravilious, C., Scharlemann, J. P. W., and Woodward, F. I.: Terrestrial carbon stocks
625 and biodiversity: key knowledge gaps and some policy implications, *Curr. Opin. Environ. Sustain.*, 2, 264–270,
626 <https://doi.org/10.1016/j.cosust.2010.05.003>, 2010.

627 Migliavacca, M., Musavi, T., Mahecha, M. D., Nelson, J. A., Knauer, J., Baldocchi, D. D., et al.: The three major axes of
628 terrestrial ecosystem function, *Nature*, 598, 468–472, <https://doi.org/10.1038/s41586-021-03939-9>, 2021.

629 Mouillot, D., Graham, N. A. J., Villéger, S., Mason, N. W. H., and Bellwood, D. R.: A functional approach reveals
630 community responses to disturbances, *Trends Ecol. Evol.*, 28, 167–175, <https://doi.org/10.1016/j.tree.2012.10.004>, 2013.

631 Mucina, L.: Biome: evolution of a crucial ecological and biogeographical concept, *New Phytol.*, 222, 97–114,
632 <https://doi.org/10.1111/nph.15609>, 2019.

633 Müller, O. V., Berbery, E. H., Alcaraz-Segura, D., and Ek, M. B.: Regional model simulations of the 2008 drought in
634 southern South America using a consistent set of land surface properties, *J. Clim.*, 27, 6754–6778,
635 <https://doi.org/10.1175/JCLI-D-13-00524.1>, 2014.

636 Myers, N., Mittermeier, R. A., Mittermeier, C. G., da Fonseca, G. A. B., and Kent, J.: Biodiversity hotspots for conservation
637 priorities, *Nature*, 403, 853–858, <https://doi.org/10.1038/35002501>, 2000.

638 Nelson, J. A., Walther, S., Gans, F., Kraft, B., Weber, U., Novick, K., et al.: X-BASE: the first terrestrial carbon and water
639 flux products from an extended data-driven scaling framework, *FLUXCOM-X*, *Biogeosciences*, 21, 5079–5115,
640 <https://doi.org/10.5194/bg-21-5079-2024>, 2024.

641 Nicholson, E., Watermeyer, K. E., Rowland, J. A., Sato, C. F., Stevenson, S. L., Andrade, A., et al.: Scientific foundations
642 for an ecosystem goal, milestones and indicators for the post-2020 global biodiversity framework, *Nat. Ecol. Evol.*, 5, 1338–
643 1349, <https://doi.org/10.1038/s41559-021-01538-5>, 2021.

644 Noss, R. F.: Indicators for monitoring biodiversity: a hierarchical approach, *Conserv. Biol.*, 4, 355–364,
645 <https://doi.org/10.1111/j.1523-1739.1990.tb00309.x>, 1990.

646 Noy-Meir, I.: Data transformations in ecological ordination: I. Some advantages of non-centering, *J. Ecol.*, 61, 329–341,
647 <https://doi.org/10.2307/2258933>, 1973.

648 Oki, T., Blyth, E. M., Berbery, E. H., and Alcaraz-Segura, D.: Land use and land cover changes and their impacts on
649 hydroclimate, ecosystems and society, in: *Climate Science for Serving Society: Research, Modeling and Prediction*
650 *Priorities*, edited by: Asrar, G. R. and Hurrell, J. W., Springer Netherlands, Dordrecht, 185–203, https://doi.org/10.1007/978-94-007-6692-1_10, 2013.

652 Pacheco-Labrador, J., Migliavacca, M., Ma, X., Mahecha, M. D., Carvalhais, N., Weber, U., et al.: Challenging the link

653 between functional and spectral diversity with radiative transfer modeling and data, *Remote Sens. Environ.*, 280, 113170,
654 <https://doi.org/10.1016/j.rse.2022.113170>, 2022.

655 Palter, J. B.: The role of the Gulf Stream in European climate, *Annu. Rev. Mar. Sci.*, 7, 113–137,
656 <https://doi.org/10.1146/annurev-marine-010814-015656>, 2015.

657 Paruelo, J. M., Jobbágy, E. G., and Sala, O. E.: Current distribution of ecosystem functional types in temperate South
658 America, *Ecosystems*, 4, 683–698, <https://doi.org/10.1007/s10021-001-0148-9>, 2001.

659 Pastorello, G., Trotta, C., Canfora, E., Chu, H., Christianson, D., Cheah, Y. W., et al.: The FLUXNET2015 dataset and the
660 ONEFlux processing pipeline for eddy covariance data, *Sci. Data*, 7, 225, <https://doi.org/10.1038/s41597-020-0534-3>, 2020.

661 Pearson, R. G. and Dawson, T. P.: Predicting the impacts of climate change on the distribution of species: are bioclimate
662 envelope models useful?, *Glob. Ecol. Biogeogr.*, 12, 361–371, <https://doi.org/10.1046/j.1466-822X.2003.00042.x>, 2003.

663 Pereira, H. M., Ferrier, S., Walters, M., Geller, G. N., Jongman, R. H. G., Scholes, R. J., et al.: Essential biodiversity
664 variables, *Science*, 339, 277–278, <https://doi.org/10.1126/science.1229931>, 2013.

665 Pérez-Hoyos, A., Martínez, B., García-Haro, F. J., Moreno, Á., and Gilabert, M. A.: Identification of ecosystem functional
666 types from coarse resolution imagery using a self-organizing map approach: a case study for Spain, *Remote Sens.*, 6, 11391–
667 11419, <https://doi.org/10.3390/rs61111391>, 2014.

668 Petrakis, S., Barba, J., Bond-Lamberty, B., and Vargas, R.: Using greenhouse gas fluxes to define soil functional types, *Plant
669 Soil*, 423, 285–294, <https://doi.org/10.1007/s11104-017-3513-2>, 2018.

670 Pettorelli, N., Böhne, H. S. to, Tulloch, A., Dubois, G., Macinnis-Ng, C., Queirós, A. M., et al.: Satellite remote sensing of
671 ecosystem functions: opportunities, challenges and way forward, *Remote Sens. Ecol. Conserv.*, 4, 71–93,
672 <https://doi.org/10.1002/rse2.59>, 2018.

673 Pettorelli, N., Wegmann, M., Skidmore, A., Múcher, S., Dawson, T. P., Fernandez, M., et al.: Framing the concept of
674 satellite remote sensing essential biodiversity variables: challenges and future directions, *Remote Sens. Ecol. Conserv.*, 2,
675 122–131, <https://doi.org/10.1002/rse2.15>, 2016.

676 Reed, R. A., Peet, R. K., Palmer, M. W., and White, P. S.: Scale dependence of vegetation-environment correlations: a case
677 study of a North Carolina piedmont woodland, *J. Veg. Sci.*, 4, 329–340, <https://doi.org/10.2307/3236104>, 1993.

678 Reichstein, M., Bahn, M., Mahecha, M. D., Kattge, J., and Baldocchi, D. D.: Linking plant and ecosystem functional
679 biogeography, *Proc. Natl. Acad. Sci. USA*, 111, 13697–13702, <https://doi.org/10.1073/pnas.1216065111>, 2014.

680 Requena-Mullor, J. M., López, E., Castro, A. J., Alcaraz-Segura, D., Castro, H., Reyes, A., and Cabello, J.: Remote-sensing
681 based approach to forecast habitat quality under climate change scenarios, *PLoS ONE*, 12, e0172107,
682 <https://doi.org/10.1371/journal.pone.0172107>, 2017.

683 Requena-Mullor, J. M., Quintas-Soriano, C., Brandt, J., Cabello, J., and Castro, A. J.: Modeling how land use legacy affects
684 the provision of ecosystem services in Mediterranean southern Spain, *Environ. Res. Lett.*, 13, 114008,
685 <https://doi.org/10.1088/1748-9326/aae00e>, 2018.

686 Richardson, K., Steffen, W., Lucht, W., Bendtsen, J., Cornell, S. E., Donges, J. F., et al.: Earth beyond six of nine planetary

687 boundaries, *Sci. Adv.*, 9, eadh2458, <https://doi.org/10.1126/sciadv.adh2458>, 2023.

688 Rocchini, D., Bacaro, G., Chirici, G., Da Re, D., Feilhauer, H., Foody, G. M., et al.: Remotely sensed spatial heterogeneity
689 as an exploratory tool for taxonomic and functional diversity study, *Ecol. Indic.*, 85, 983–990,
690 <https://doi.org/10.1016/j.ecolind.2017.11.052>, 2018.

691 Rosenzweig, C. and Dickinson, R. (eds.): *Climate-Vegetation Interactions*, Office for Interdisciplinary Earth Studies,
692 University Corporation for Atmospheric Research, Boulder, CO, USA, 1986.

693 Running, S. W., Baldocchi, D. D., Turner, D. P., Gower, S. T., Bakwin, P. S., and Hibbard, K. A.: A global terrestrial
694 monitoring network integrating tower fluxes, flask sampling, ecosystem modeling and EOS satellite data, *Remote Sens.*
695 *Environ.*, 70, 108–127, [https://doi.org/10.1016/S0034-4257\(99\)00061-9](https://doi.org/10.1016/S0034-4257(99)00061-9), 1999.

696 Running, S. W., Nemani, R. R., Heinsch, F. A., Zhao, M., Reeves, M., and Hashimoto, H.: A continuous satellite-derived
697 measure of global terrestrial primary production, *BioScience*, 54, 547–560, [https://doi.org/10.1641/0006-3568\(2004\)054\[0547:ACSMOG\]2.0.CO;2](https://doi.org/10.1641/0006-3568(2004)054[0547:ACSMOG]2.0.CO;2), 2004.

699 Saccone, P., Hoikka, K., and Virtanen, R.: What if plant functional types conceal species-specific responses to environment?
700 Study on arctic shrub communities, *Ecology*, 98, 1600–1612, <https://doi.org/10.1002/ecy.1822>, 2017.

701 Skidmore, A. K., Coops, N. C., Neinavaz, E., Ali, A., Schaepman, M. E., Paganini, M., et al.: Priority list of biodiversity
702 metrics to observe from space, *Nat. Ecol. Evol.*, 5, 896–906, <https://doi.org/10.1038/s41559-021-01451-y>, 2021.

703 Skidmore, A. K., Pettorelli, N., Coops, N. C., Geller, G. N., Hansen, M., Lucas, R., ... & Wegmann, M. Environmental
704 science: Agree on biodiversity metrics to track from space. *Nature*, 523(7561), 403-405. <https://doi.org/10.1038/523403a>,
705 2015.

706 Steffen, W., Richardson, K., Rockström, J., Cornell, S. E., Fetzer, I., Bennett, E. M., et al.: Planetary boundaries: guiding
707 human development on a changing planet, *Science*, 347, 1259855, <https://doi.org/10.1126/science.1259855>, 2015.

708 Suding, K. N. and Goldstein, L. J.: Testing the Holy Grail framework: using functional traits to predict ecosystem change,
709 *New Phytol.*, 180, 559–562, <https://doi.org/10.1111/j.1469-8137.2008.02667.x>, 2008.

710 Sundseth, K.: Natura 2000 in the Alpine region, European Commission, <https://doi.org/10.2779/84763>, 2009a.

711 Sundseth, K.: Natura 2000 in the Continental region, European Commission, <https://doi.org/10.2779/29261>, 2009b.

712 Thomas, H. J. D., Myers-Smith, I. H., Bjorkman, A. D., Elmendorf, S. C., Blok, D., Cornelissen, J. H. C., et al.: Traditional
713 plant functional groups explain variation in economic but not size-related traits across the tundra biome, *Glob. Ecol.*
714 *Biogeogr.*, 28, 78–95, <https://doi.org/10.1111/geb.12856>, 2019.

715 Tilman, D., Isbell, F., and Cowles, J. M.: Biodiversity and ecosystem functioning, *Annu. Rev. Ecol. Evol. Syst.*, 45, 471–
716 493, <https://doi.org/10.1146/annurev-ecolsys-120213-091917>, 2014.

717 Vargas, R., Sonnentag, O., Abramowitz, G., Carrara, A., Chen, J. M., Ciais, P., et al.: Drought influences the accuracy of
718 simulated ecosystem fluxes: a model-data meta-analysis for Mediterranean oak woodlands, *Ecosystems*, 16, 749–764,
719 <https://doi.org/10.1007/s10021-013-9648-1>, 2013.

720 Vaz, A. S., Alcaraz-Segura, D., Campos, J. C., Vicente, J. R., and Honrado, J. P.: Managing plant invasions through the lens

721 of remote sensing: a review of progress and the way forward, *Sci. Total Environ.*, 642, 1328–1339,
722 <https://doi.org/10.1016/j.scitotenv.2018.06.142>, 2018.

723 Villarreal, S., Guevara, M., Alcaraz-Segura, D., and Vargas, R.: Optimizing an environmental observatory network design
724 using publicly available data, *J. Geophys. Res. Biogeosci.*, 124, 1812–1826, <https://doi.org/10.1029/2018JG004776>, 2019.

725 Villarreal, S., Guevara, M., Alcaraz-Segura, D., Brunzell, N. A., Hayes, D., Loescher, H. W., and Vargas, R.: Ecosystem
726 functional diversity and the representativeness of environmental networks across the conterminous United States, *Agric. For.
727 Meteorol.*, 262, 423–433, <https://doi.org/10.1016/j.agrformet.2018.07.026>, 2018.

728 Villarreal, S. and Vargas, R.: Representativeness of FLUXNET sites across Latin America, *J. Geophys. Res. Biogeosci.*,
729 126, e2020JG006090, <https://doi.org/10.1029/2020JG006090>, 2021.

730 Villarreal, S. and Vargas, R.: Representativeness of FLUXNET sites across Latin America, *J. Geophys. Res. Biogeosci.*,
731 126, e2020JG006090, <https://doi.org/10.1029/2020JG006090>, 2021.

732 Violle, C., Reich, P. B., Pacala, S. W., Enquist, B. J., and Kattge, J.: The emergence and promise of functional biogeography,
733 *Proc. Natl. Acad. Sci. USA*, 111, 13690–13696, <https://doi.org/10.1073/pnas.1415442111>, 2014.

734 Violle, C., Thuiller, W., Mouquet, N., Munoz, F., Kraft, N. J. B., Cadotte, M. W., Livingstone, S. W., and Mouillot, D.:
735 Functional rarity: the ecology of outliers, *Trends Ecol. Evol.*, 32, 356–367, <https://doi.org/10.1016/j.tree.2017.02.002>, 2017.

736 Virginia, R. A. and Wall, D. H.: Ecosystem function, principles of, in: *Encyclopedia of Biodiversity*, edited by: Levin, S. A.,
737 Academic Press, San Diego, 345–352, <https://doi.org/10.1016/B978-0-12-384719-5.00031-0>, 2001.

738 Vitousek, P. M.: Beyond global warming: ecology and global change, *Ecology*, 75, 1861–1876,
739 <https://doi.org/10.2307/1941591>, 1994.

740 Wang, L., Zhu, H., Lin, A., Zou, L., Qin, W., and Du, Q.: Evaluation of the latest MODIS GPP products across multiple
741 biomes using global eddy covariance flux data, *Remote Sens.*, 9, 418, <https://doi.org/10.3390/rs9050418>, 2017.

742 Whittaker, R. J., Nogués-Bravo, D., and Araújo, M. B.: Geographical gradients of species richness: a test of the water–
743 energy conjecture of Hawkins et al. (2003) using European data for five taxa, *Glob. Ecol. Biogeogr.*, 16, 76–89,
744 <https://doi.org/10.1111/j.1466-822X.2006.00268.x>, 2007.

745 Williams, B. K.: Discriminant analysis in wildlife research: theory and applications, in: *The Use of Multivariate Statistics in
746 Studies of Wildlife Habitat*, edited by: Capen, D. E., 59–71, General Technical Report RM-87, U.S. Department of
747 Agriculture, Forest Service, 1981.

748 Williams, B. K.: Some observations of the use of discriminant analysis in ecology, *Ecology*, 64, 1283–1291,
749 <https://doi.org/10.2307/1937839>, 1983.

750 Wullschleger, S. D., Epstein, H. E., Box, E. O., Euskirchen, E. S., Goswami, S., Iversen, C. M., Kattge, J., Norby, R. J., van
751 Bodegom, P. M., and Xu, X.: Plant functional types in Earth system models: past experiences and future directions for
752 application of dynamic vegetation models in high-latitude ecosystems, *Ann. Bot.*, 114, 1–16,
753 <https://doi.org/10.1093/aob/mcu077>, 2014.

754 Xiao, H., McDonald-Madden, E., Sabbadin, R., Peyrard, N., Dee, L. E., and Chadés, I. The value of understanding feedbacks
755 from ecosystem functions to species for managing ecosystems. *Nature Communications*, 10(1),
756 3901.<https://doi.org/10.1038/s41467-019-11890-7>, 2019.

757 Zhang, Y., Song, C., Sun, G., Band, L. E., McNulty, S., Noormets, A., Zhang, Q., and Zhang, Z.: Development of a coupled
758 carbon and water model for estimating global gross primary productivity and evapotranspiration based on eddy flux and
759 remote sensing data, *Agric. For. Meteorol.*, 223, 116–131, <https://doi.org/10.1016/j.agrformet.2016.04.019>, 2016.

760

761 **Biosketch**

762 Beatriz Cazorla is a postdoc whose research focuses on remotely sensed ecosystem functioning at regional scales, their
763 conservation, and their relationship with global change. All other authors are expert in ecosystem functioning, remote sensing,
764 regional ecology, biogeography or energy fluxes.